

Efficient Flow Control in Industrial Processes: Estimating In-flow at Control Valves Without Physical Sensors

Bhagya R Navada¹, Santhosh Krishnan Venkata^{2*}, Preeti Mohanty³

^{1, 2, 3} Centre for Cyber Physical System, Department of Instrumentation and Control, Manipal Institute of Technology, Manipal Academy of Higher Education, Manipal, India

Email: ¹ kgbagya@gmail.com, ² santhu.kv@gmail.com, ³ mohanty.preeti@manipal.edu

*Corresponding Author

Abstract—In industrial processes, achieving an efficient flow is paramount as various loops are controlled through flow control. To optimize this flow, it is essential to monitor various influential components such as control valves, flow sensors, as well as input and output parameters to the valve. To maintain the desired flow rate at the outlet of the control valve, it's imperative that the valve's inflow remains higher than the desired output flow rate. In most applications, fluctuations in the inflow rate are typically not considered as a significant factor affecting changes in the output flow which is a key driving component leading to our research objective. This research paper's contribution is estimation of control valve's inlet flow rate without the need for physical sensors and validation of estimated flow rate. This estimator relies on an outflow measurement from an orifice flow meter and employs a first order process with dead time model to deduce the inflow to the control valve. The process model is formulated through data driven system identification, employing the input-output characteristics of the system. Furthermore, a pole-placement-based estimator is developed utilizing real-world data. The novelty of the approach is estimation of the flow rate at valve input which is overlooked by many researchers. To validate the performance of this estimator, it is deployed to compute the inflow in a real-life practical system. The results reveal a root mean square error of 0.029, signifying the accuracy and reliability of the designed estimator. The estimator performed better in terms of reduced root mean square error when compared to other methods.

Keywords—Control Valve; Estimation; Inflow; Soft Sensor; Flow; Pneumatic Actuator; Flow Rate; Pole Placement.

I. INTRODUCTION

Industries have become major contributors in fulfilling the fundamental requirements of individuals in day-to-day life [1][2]. Hence, extreme competition exists among industries to deliver better products. To achieve accurate and fast production without compromising product quality, monitoring industrial processes is essential [3][4]. Thus, to monitor industrial processes, several parameters, such as pressure, humidity, temperature, level, flow, and viscosity, need to be measured. These parameters can be measured using diverse principles via contact- and noncontact-type methods [5]. In particular, the flow rate is an important parameter in many industries, including chemical [6][7], food [8][9][10], iron and steel [11][12], pharmaceutical [13][14], pulp and paper [15][16], oil and gas [17][18] industries, to control material flow and seed flow [19][20]. Therefore,

measuring fluid flow is imperative in many industries to maintain the control variable in a specified range.

Several methods are available for measuring the fluid flow rate. Head-type flow meters, namely orifice, and venturi, are the most commonly used flow meters. Electromagnetic flow meters are used when the fluid is conductive, and ultrasonic flow meters [21][22] are primarily used when a noninvasive method of flow measurement technique is needed, such as blood flow measurement [23]. Orifice meters are used because of their benefits, such as simplicity, ruggedness, and cost-effectiveness [24][25], while venturi meters are used because of their good accuracy and reliability [26][27]. In [28], the differential ultrasonic transmission time was considered for the measurement of flow rate in a small diameter pipe using digital signal processing techniques. The aforementioned works emphasize the use of physical sensor for general parameter measurement. However, several other methods of flow rate measurement exist that have been designed for specific applications; some of these methods are highlighted in the following paragraph.

The flow rate is measured according to a Bragg grating method using a differential optical fiber probe. This method is utilized when a large range of flow measurements is required [29]. A fringing field capacitor that showed a change in capacitance in response to a change in fluid flow was used to monitor the flow in [30]. An annular capacitor is built on the tube surface to provide fringing capacitance. In [31], the flow rate was measured using a Hall probe sensor that utilizes a magnetic float to measure the flow rate variation. The Hall probe sensor measures the magnetic intensity, which is a function of the distance between the magnetic float and the Hall probe sensor. Piezoelectric sensors are used to measure the flow rate in straight and bent pipes by measuring variations in pressure [32]. Furthermore, piezoelectric accelerometers are used to measure the flow rate through the vibrations created by the fluid particles. This method does not disturb the physical flow, as there is no hindrance to the fluid flow [33]. A polyvinylidene fluoride film sensor that functions based on the piezoelectric principle is used to measure the fluid flow rate [34]. The flow rate is indirectly measured by measuring the response to some chemical reactions that are a function of the change in the flow rate [35]. Radiotracers such as iodine 131 have been used to measure the flow rate in large pipes by measuring the tracer



concentration [36]. The flow rate can be measured using a bare laser diode as an interferometer. However, this method is unsuitable for pure water because it requires liquids that allow optical scattering [37]. Furthermore, nonsymmetric flow profiles can be measured at several positions in the flow cross-section using a thermal anemometry grid sensor [38]. Flow at different depths in a vessel can be measured using a low-coherence interferometer [39]. The reported works discussed here are used to specific applications signifying their limitations.

These are the applications that are covered here when direct contact with the sensor is not feasible. Noncontact type flow measurement techniques such as using an image sensor have been employed to estimate the real flow where isolation is essential [40]. For noncontact-type flow measurements, luminescent diode interferometers have also been used [41]. In this method, the flow rate is calculated based on the measured Doppler spectrum from the moving particles in the pipe. The flow rate of fluid and solid without obstructing the flow is reported in [42] using the Doppler effect. The industries also require measurement of the solid feed flow rate, and Doppler radar is used for the same in [43].

To understand the behavior of any system, knowing the significant system variables is essential, which in most situations are measured using suitable sensors [44]. Industrial processes will have multiple loops involved and each loop comprises of various parameters of concern which requires plant wise process monitoring [45]. This requires several sensors to measure various process parameters. However, in some situations, the placement of physical sensors has several constraints; thus, the direct measurement of these parameters is very complicated. Hence, these parameters must be indirectly assessed by measuring other parameters associated with the required parameter [46][47]. This process of indirect measurement is known as estimation or soft sensing [48][49].

The flow estimation methods support in the process of industrial process monitoring thus making them vital requirements of the industrial process [50]. This section details some of the flow estimation methods. The flow rate of the water pumping system was estimated in [51] using an artificial neural network model based on hourly temperature and solar irradiation measurements. A data-driven soft sensor that uses information about water level from an inexpensive ultrasonic distance sensor to estimate wastewater flowrate is detailed in [52]. The flow rate in a pipe was estimated by measuring the pipe vibration using a single-axis accelerometer [53]. Here, the flow rate was measured without causing any disturbance to the fluid flow. In [54], design and testing of several soft sensing methods for estimating flow rate, such as software-based sensors that make use of the relationship between hydraulic spool valve flow force and flow rate is reported.

In [55], the inflow rate to the control valve was estimated using a soft sensor. This soft sensor was developed based on the control signal and output flow rate measurements using pole placement and Kalman filtering-based observer design methods. The river fluid motion was estimated using an image-based flow sensor in [56]. Therein, the estimated motion data were three-dimensional river top layer gesture

data. The fluid velocity was estimated in [57] to support cancer diagnosis from ultrasound poroelastography, wherein a filter was designed to eliminate the noise in the images to estimate the fluid velocity.

In process industries, multiple loops are in need of control of the vital parameters and one of them that requires major attention is fluid flow [58]. Controlling of all the loop variables is imperative in industrial processes to attain better and accurate quality of final product [59]. These flow parameters are controlled using pneumatic control valves as final control elements. The inclusion of control valve majorly affects the pattern of fluid flow at the output of the valve as it introduces the nonlinearity and also two-way behavior while opening and closing of the control valve leading to nonlinear variation of flow rate at the valve output.

Literatures highlight the significance of flow process in industrial processes. Many flow rate measurement techniques have been specified, and some of them are application specific. In several methods, physical sensors are predominantly used which is not suitable in all the scenarios. Thus gaps identified are non-suitability of the sensors for various flow measurement applications due to the limitation of size, applicability, cost and the place of measurement. As the output flow rate is influenced by the input flow to the control valve, hence requires measurement. However, it requires additional sensors, which increases the complexity and cost of the monitoring system. A nonphysical sensor could be used to replace the need for hard sensors, which would simplify and lower the expense. Our study aims to develop a soft sensor to measure inflow to the control valve using a continuous observer. The research contribution of this study is in developing a cost effective estimator for the measurement of inflow to the control valve and validating the results with real life implementations. This estimator is suitable to incorporate in flow control loops involving pneumatic actuator as the final control element. On the other hand, given the dynamics of the process, the process model needs to be adjusted.

The remainder of this paper is organized as follows. First, the problem statement is presented. Then, the experimental setup is detailed, and the system model identification is elaborated. Finally, the obtained results are highlighted, and the conclusions are presented.

II. PROBLEM STATEMENT MATERIALS AND METHODS

The flow control loop is the principally used control loop in most industrial processes. Valve output flow rate is an influential parameter in industrial processes as it is in direct contact with the process thus any abrupt changes in this would affect the process. However, the shift in the output flow rate depends on the movement of the control valve stem as well as input flow rate to the control valve. Thus, determining the inflow rate is necessary while monitoring the flow process with a penalty of increased monitoring cost. Therefore, this study aims to design a soft sensor to measure the inflow to the pneumatic control valve used in a flow process. The major contribution of the work is estimation of inflow to the control valve, which helps to prevent inaccurate diagnosis during the monitoring procedure. The graphical representation of the overall work is presented in Fig. 1

highlighting the process of estimator design for the measurement of inflow to the control valve. Inflow detection was not considered an influential parameter for control valve health monitoring. The major application includes health monitoring of the control valve, facilitating precise data even at the time of failure of real sensor. Here, the main requirement is to identify the abnormal behavior of the control valve by observing the valve output in terms of the output flow rate. Change in the valve output flow rate is a function of both inflow and valve movement. An unexpected change in output flow rate for a known valve movement indicates that the actuator is malfunctioning, however in actual scenario this is a false alarm. This misleading observation can be avoided by estimating the change in the input flow rate [60].

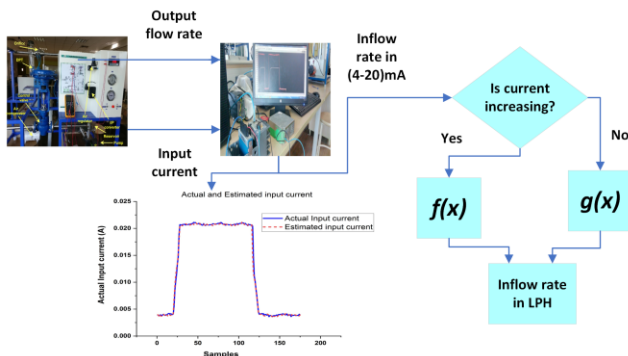


Fig. 1. Graphical abstract

III. EXPERIMENTAL SETUP

The flow process station considered in this study is represented in Fig. 2. A pneumatic control valve is used as the final control element that controls the inflow. The control valve is manufactured by R. K. Control Instruments Pvt. Ltd. The C_v of the control valve provided by the manufacturer is 5. The control valve used is an equal percentage and air to open type valve; thus, normally it will be in the closed position.

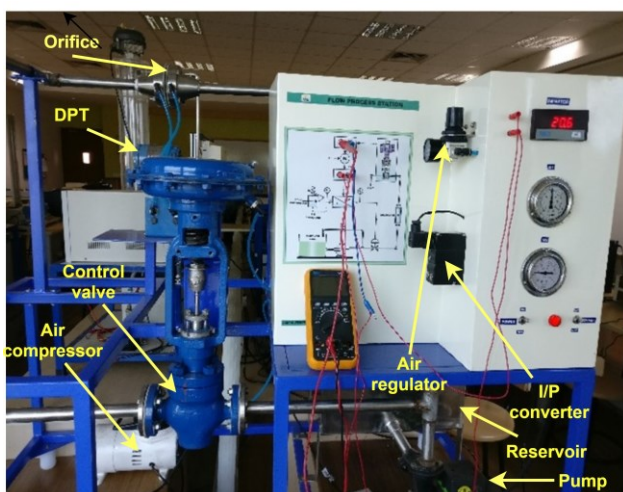


Fig. 2. Experimental setup

The Piping and Instrumentation (P&I) diagram of the flow process is shown in Fig. 3. The flow process comprises a reservoir, pump, rotameter, orifice meter, Electro-Magnetic (EM) flow meter, and a control valve. The pump has a

maximum of 1800 rpm, rotameter has a maximum scale up to 1000 LPH. The orifice with a differential pressure transmitter (DPT) is placed at the valve outlet to measure the valve output flow rate and represent it as a current in the 4–20 mA range for an input variation of 0–1000LPH. Water flows through the EM flow meter, control valve, rotameter, and orifice and then back to the reservoir, as shown in Fig. 3. The dashed and dotted lines in the Fig. 3 denote the water flow and compressed air flow, respectively. The EM flow meter is connected to the control valve inlet to measure the inflow rate. The bypass valve is placed near the pump to provide a path for the fluid when the control valve is not fully open.

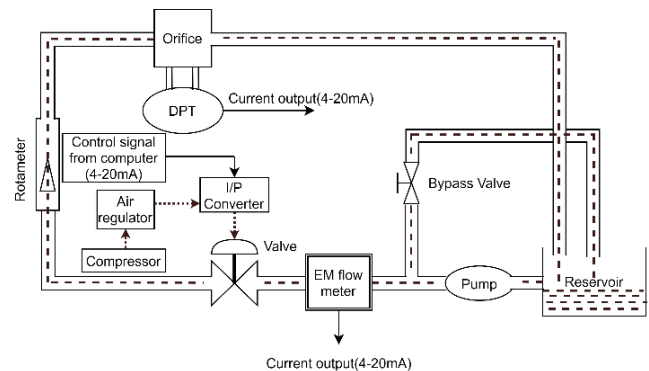


Fig. 3. P & I diagram of the flow process

An input current of 4–20 mA range is applied to the current to pressure (I/P) converter to drive the operation of control valve. The I/P converter transforms 4–20mA of current into a pressure signal with a range of 3–15 psi, provided the supply pressure is maintained above the required range. An air compressor is included to supply the pressure required by the I/P converter. The pressure regulator maintains the compressed air at a level above 15 psi, which is normally maintained at 20 psi. When the control valve opens, the fluid passes through a rotameter and an orifice before returning to the reservoir. The control valve opens more as the control signal rises, increasing the valve outflow, which is evidenced by the rising current at the DPT output.

To analyze the system behavior, the system input and output need to be observed. Here, the control valve is considered as the system with the control signal in 4–20mA range as the input and the DPT output in 4–20mA range as output. To transmit input and output signals to the computer, data acquisition devices that support the type and range of the signals are necessary. Hence, NI c-RIO 9012 with a reconfigurable integrated chassis with eight slots is employed as the acquisition device. It has one Ethernet port and one RS-232 serial port for communication. The c-RIO is powered through a 9–35 V DC supply, has 64 MB of memory with a processing speed of 400MHz. The current input module NI 9203 installed in the NI c-RIO 9012 chassis is utilized as the acquisition device to acquire the control input and output flow rate represented in current ranging from 4 to 20 mA.

To estimate the inflow to the control valve, the process model needs to be obtained, which can be obtained by analyzing the input and output of the control valve. The input to the control valve stem movement is the control input current ranging from 4 to 20 mA, which causes a variation in the valve stem movement and subsequently causes a change

in the output flow rate. In this process, the control input to the control valve is operated manually. A continuous variation of control input manually resulted in change in DPT output. One analog current input channel of NI 9203 is connected to control input signal and another channel is connected to DPT output. The NI c-RIO 9012 is connected to the computer through Ethernet cable through which serial communication is achieved. NI c-RIO 9012 is configured with IP address on the same subnet and gateway as that of the system with LabVIEW software. Set of these input and output parameters are acquired in the LabVIEW project for further analysis and estimator design as shown in Fig. 4. It is also observed from the figure that a set of input and output signals have been acquired and plotted on the LabVIEW chart.

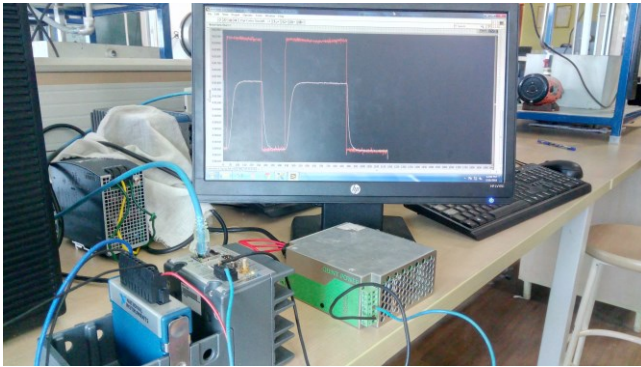


Fig. 4. The interface of c-RIO to the computer with input and output data

IV. IDENTIFICATION OF SYSTEM MODEL

To develop an observer-based estimator, a system transfer function is required to understand the flow process dynamics. The flow process system transfer function is determined by considering the control input to the I/P converter as the input parameter and the valve output flow rate as the output parameter. To obtain the system transfer function, a set of input and output data is acquired into the computer using c-RIO 9012 and the current input module NI 9203. The data thus acquired is then imported into the MATLAB system identification toolbox. As the valve nonlinearity is represented to be a first order system with a dead time, same system format is selected in identification toolbox. While performing system identification, the initial conditions are set to backcast, and several iterations were performed and the best fit obtained is 95% fit, as displayed in Fig. 5.

The transfer function stemming from the system identification toolbox is as follows:

$$P(s) = \frac{0.615}{20s + 1} e^{-10s} \quad (1)$$

As the practical system is considered to have a small bias of 0.00159, it is added to the transfer function given in equation (1), yielding the transfer function in equation (2). The estimator design process in LabVIEW platform requires the model to be represented in state space form. To represent (2) in the state-space form, the delay element needs to be eliminated, which could be achieved through time series expansion using Pade approximation. The first order system is now changed to second order system by transforming the

delay element with first order system into the second order system transfer function given in equation (3).

$$P(s) = \frac{0.615}{20s + 1} e^{-10s} + 0.00159 \quad (2)$$

$$P(s) = \frac{0.0318s^3 + 0.6357s^2 - 0.364s + 0.0739}{20s^3 + 13s^2 + 3s + 0.12} \quad (3)$$

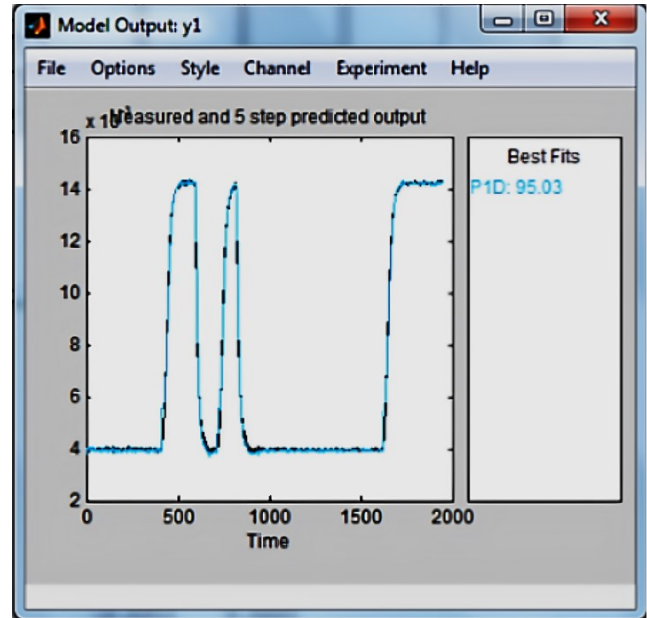


Fig. 5. Estimated transfer function with a 95% fit

Equation (3) stems from (2) because of the bias element and the approximated delay. Now the second order system transfer function is converted into a state space approximation with three states and the state-space system, input and output matrices as represented below.

$$A = \begin{bmatrix} -0.65006 & -0.300012 & -0.0960038 \\ 0.5 & 0 & 0 \\ 0 & 0.125 & 0 \end{bmatrix}; B = \begin{bmatrix} 4 \\ 0 \\ 0 \end{bmatrix};$$

$$C = [0.00768 \quad 0.00922 \quad 0.01476]; D = [0.00159]$$

Where, A is State matrix, B is Input matrix, C is output matrix, D is feedthrough matrix.

A. Inflow Estimation

The inflow to the control valve significantly influences the range of the flow rate at the control valve output. The proposed system aims to determine the inflow to the control valve such that the actual cause of variation in the output flow rate can be spotted. The output flow variation could be because of a change in the stem displacement or the input flow rate; thus, if the inflow rate is known, the valve stem displacement and the output flow rate can be directly related. Here, the input current is estimated, and then the input current is mapped to the input flow rate.

An observer design is a dynamic method to estimate the state. The state of the system is estimated based on the system input and output data. For a given system, an observer can be

designed only if the given system is stable, observable, and controllable. The state-space model of the system given in (3) satisfies the controllability, observability, and stability requirements.

The block diagram of the estimator is shown in Fig. 6. As represented in the diagram, the system states ' \hat{x} ' and the system outputs ' \hat{y} ' are estimated based on the input signal ' u ', and the system output ' y '. System input, states, and output are vectors representing the number of inputs, states and output values.

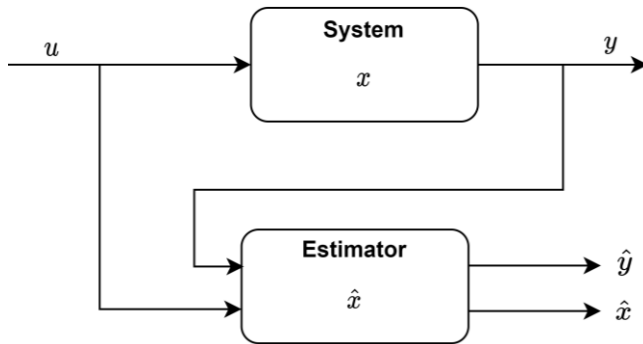


Fig. 6. Block diagram of the estimator

B. Continuous Observer

A continuous observer is an estimator working in continuous time for varying time instances. To develop an estimator that works in real life scenario, NI c-RIO 9012 is employed which work on FPGA platform. An FPGA project is created in LabVIEW, and the required target NI c-RIO 9012 is added with chassis 9101. A simulation program specified to be a virtual instrument is programmed so that the input and output currents can be imported into the program. To develop the estimator for inflow estimation with a real-life system, the continuous observer available in the LabVIEW control simulation toolbox is used [61]. This block requires the input, output, estimator gain, and system state-space model. In this function, the observer estimates the state by solving the differential equations given below.

$$\dot{\hat{x}}(t) = A\hat{x}(t) + Bu(t) + L[y(t) - \hat{y}(t)] \quad (4)$$

$$\hat{y}(t) = C\hat{x}(t) + Du(t) \quad (5)$$

In this case, the pole placement function is used to determine the estimator gain. The closed-loop estimator design method is used to place the poles at the desired locations. The observer gain is calculated for the poles $P = -0.001 + 0.197i$, $-0.001 - 0.197i$, and -0.12 , and the obtained observer gain is $L = [-25 \ 30 \ -4]^T$. For the calculated gain values, the designed estimator tracks the actual values, as represented in Fig. 7. The estimator thus estimates the valve output flow rate and the states of the system. Valve inflow rate is one of the states estimated by the observer. The estimated valve inflow and the outflow are current values ranging between 4 and 20 mA, which is then mapped to the input flow rate in LPH. This is because the input flow rate is directly proportional to the control input, i.e., current input to the I/P converter.

V. RESULTS AND ANALYSIS

The developed estimator yielded satisfactory results when it was tested with the real-life system, as shown in Fig. 7. Fig. 7 (a) represents the plot of one set of readings, and Fig. 7 (b) represents the screen shot of the output obtained for the other set of data. As mentioned earlier, the input current is computed first by measuring the control input and output flow rates, which are represented as currents ranging from 4 to 20 mA. The inflow rate variation for the input current variation is not linear due to the nonlinear behavior of the control valve. Hence, the input flow rate was measured using an electromagnetic flow meter for both increasing and decreasing control inputs. Fig. 8 displays the variation in the measured input flow rate with increasing and decreasing control input.

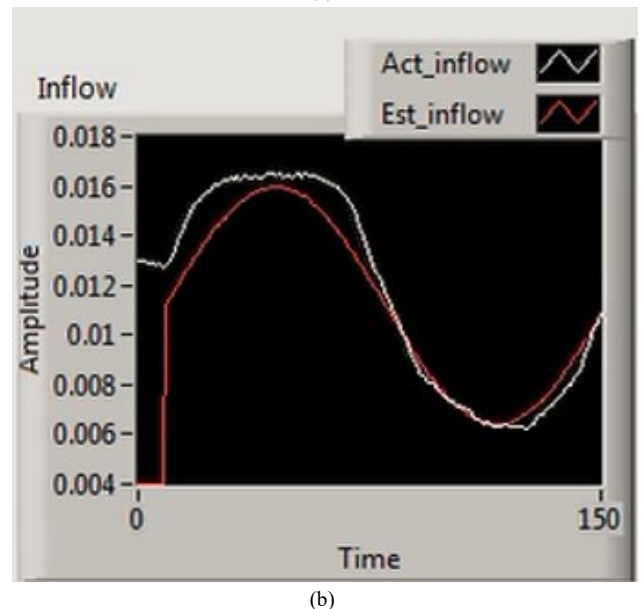
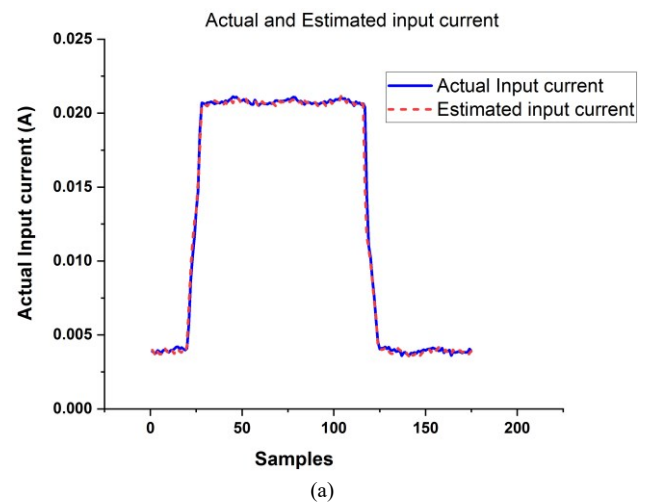


Fig. 7. Estimator output tracking the control input: (a) plotted graph and (b) screenshot of the front panel

Table I illustrates the measured inflow rate values for increasing and decreasing input currents, from which the nonuniformity of the flow rate between increasing and decreasing current values is evident. One representation cannot be used for current to flow mapping due to the nonuniformity of the variance with increasing and decreasing

flow rates. Hence, the equations for increasing and decreasing current variations are considered separately. A polynomial curve-fitting method is used to obtain the close mapping of these values. The regression order of the polynomial is selected to be 3 as the increment in order did not result in significant improvement. Therefore, the flow rate close fits obtained for increasing and decreasing currents are represented mathematically by equations (6) and (7), respectively.

TABLE I. MEASURED INPUT CURRENT WITH THE INPUT FLOW RATE FOR INCREASING AND DECREASING CURRENT INPUTS

| Input Current (mA) | Input Flowrate(lph) for 20-4mA | Input Flowrate(lph) for 4-20mA |
|--------------------|--------------------------------|--------------------------------|
| 4 | 87 | 57 |
| 6 | 162 | 57 |
| 8 | 250 | 130 |
| 10 | 370 | 234 |
| 12 | 480 | 392 |
| 14 | 625 | 530 |
| 16 | 712 | 672 |
| 18 | 738 | 727 |
| 20 | 741 | 745 |

$$g(x) = -4.928 \times 10^8 x^3 + 1.798 \times 10^7 x^2 - 1.44 \times 10^5 x + 378.9 \quad (6)$$

$$f(x) = -2.835 \times 10^8 x^3 + 8.88 \times 10^6 x^2 - 3.123 \times 10^4 x + 81.23 \quad (7)$$

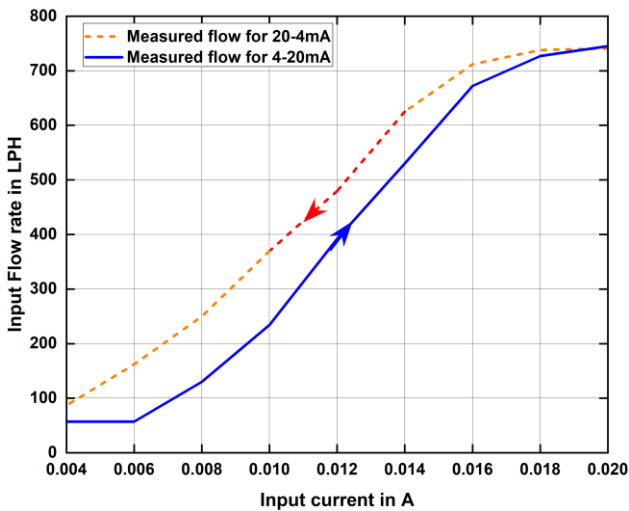


Fig. 8. Variation in the input flow rate with increasing and decreasing input current

The input flow rate corresponding to increasing current input is estimated using equation (7). The percentage error between the actual and estimated input flow rate values is shown in Table II. A maximum percentage error of 5% of the full scale is obtained for the tabulated values. The main source of error is irregularity involved in the valve movement mainly for lower flow rates. Thus the reduction in error can be achieved only if the valve movements are strictly following the required pattern. Fig. 9 displays a graph of the actual and estimated flow rates for increasing current input exhibiting the close mapping of $g(x)$ with the actual values.

TABLE II. PERCENTAGE ERROR BETWEEN THE ACTUAL AND ESTIMATED INPUT FLOW RATES USING THE POLYNOMIAL $G(X)$ FOR INCREASING CURRENT INPUT FROM 4 TO 20 MA

| Input Current (mA) | Input Flowrate(lph) for 4-20 mA | Estimated Flowrate(lph) for $g(x)$ | % error |
|--------------------|---------------------------------|------------------------------------|---------|
| 4 | 57 | 59 | -3.50 |
| 6 | 57 | 55 | 3.50 |
| 8 | 130 | 125 | 3.84 |
| 10 | 234 | 244 | -4.27 |
| 12 | 392 | 388 | 1.02 |
| 14 | 530 | 534 | -0.75 |
| 16 | 672 | 659 | 1.93 |
| 18 | 727 | 738 | -1.51 |
| 20 | 745 | 749 | -0.53 |

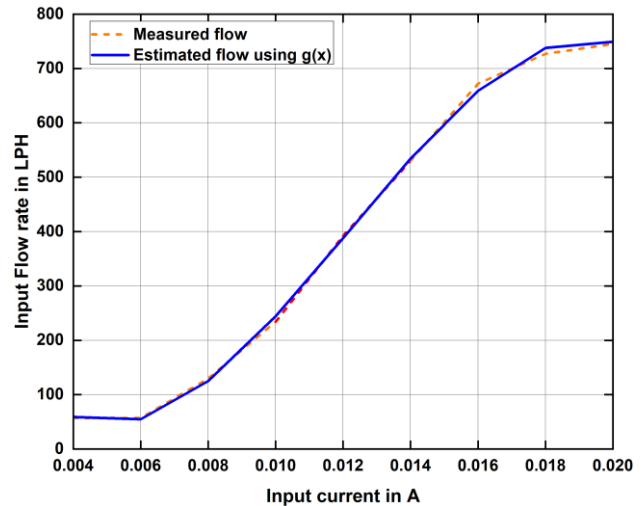


Fig. 9. The actual values and the estimated input flow rate using the polynomial $g(x)$ for increasing current input

The input flow rate corresponding to decreasing current input is estimated using equation (8), and the percentage error between the actual and estimated input flow rates is shown in Table III. A graph of the actual and estimated flow rates for decreasing current input is depicted in Fig. 10, which also shows how closely the actual values and $f(x)$ map. Thus, by observing the mode of input change, suitable mapping equations are selected to map the estimated current to the input flow rate.

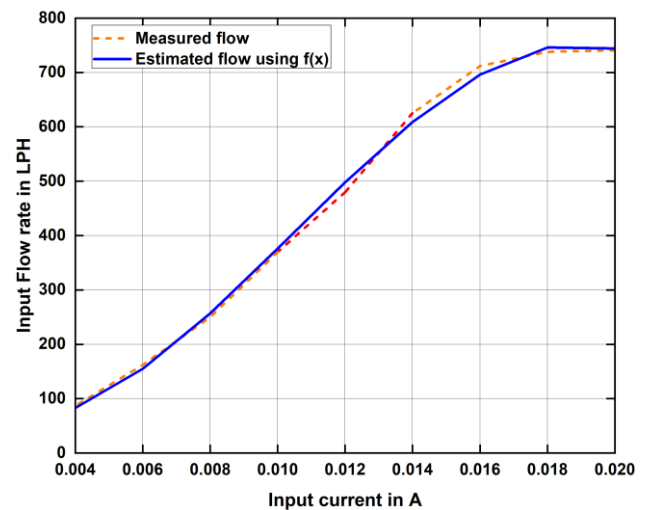


Fig. 10. Actual values and the estimated input flow rate using the polynomial $f(x)$ for decreasing current input

The estimated values obtained through this method are compared with the artificial neural network-based estimation method [51]. As the flow rate mentioned in [51] was represented in m³/hour, the present work measurements were also converted into m³/hour. The root-mean square error for the technique reported in [51] is 0.33, whereas for the proposed method, it is 0.0072, thus signifying the better performance of the proposed method. The improvement in the proposed estimator is mainly due to its adaptation toward the variation with increasing and decreasing current input.

TABLE III. PERCENTAGE ERROR BETWEEN THE ACTUAL AND ESTIMATED INPUT FLOW RATES USING THE POLYNOMIAL G(X) FOR INCREASING CURRENT INPUT FROM 4 TO 20 MA

| Input Current (mA) | Input Flowrate(lph) for 20-4mA | Estimated Flowrate(lph) for f(x) | % error |
|--------------------|--------------------------------|----------------------------------|---------|
| 20 | 741 | 744 | -0.40 |
| 18 | 738 | 746 | -1.08 |
| 16 | 712 | 696 | 2.24 |
| 14 | 625 | 609 | 2.56 |
| 12 | 480 | 498 | -3.75 |
| 10 | 370 | 376 | -1.62 |
| 8 | 250 | 257 | -2.80 |
| 6 | 162 | 155 | 4.32 |
| 4 | 87 | 83 | 4.59 |

VI. CONCLUSION

The flow process is invariably employed in all process industries, and the control valve is an important element of the flow process, which is employed to modify the flow rate based on the desired set points. If the flow rate at the valve inlet varies, then the outlet flow has an error even with the appropriate functioning of the control valve. To ensure that the inlet flow is at the desired flow, an additional flow sensor needs to be provided, which is not always a feasible solution due to placement and economic constraints. The contribution of this research work comprises design of estimator for prediction of inlet flow rate of the control valve. The validation of the estimator also is added contribution to the work. The designed estimator values have been validated by deploying the soft sensor onto the real life system and comparing the estimated values with the actual measured values. Thus, this study aimed to design an estimator to estimate the flow rate at the inlet using the characteristics of the process parameters. The process model is identified by using system identification toolbox of the MATLAB. First order system with dead time process model pattern is selected in the tool and the initial conditions were selected as back cast. The working of the estimator is analyzed for both increasing and decreasing current variations with different polynomials used for mapping the current inputs to the estimated flow rates in LPH. In both the cases, a maximum percentage error of 5% was observed from the result. The estimator performance was validated by comparing the estimated inflow with the actual values obtained from the EM flow meter. The estimator output yielded a root mean square error of 0.029, demonstrating the reliability of the designed estimator. The higher accuracy can be explained by comparing the root mean square error of the suggested strategy (about 0.0072) with the estimating technique published in [51], which had a root mean square error of 0.33. These estimated values can be considered an influencing

parameter in the process of control valve fault detection. As these values inform the user about the root cause for the change in valve output flow rate, false alarming rate of control valve faults can be lowered. The limitation of the work is that the designed estimator can be incorporated only in the flow loops with pneumatic actuator as the final control element. The future scope of this work includes improvement of the performance of the estimator by incorporating data fusion techniques.

REFERENCES

- [1] E. Valette, H.B. El-Haouzi, and G. Demesure, "Industry 5.0 and its technologies: A systematic literature review upon the human place into IoT-and CPS-based industrial systems," *Computers & Industrial Engineering*, vol. 184, p. 109426, 2023, doi: 10.1016/j.cie.2023.109426.
- [2] M. T. Wolfe and P. C. Patel, "Same Difference? The impact of Low-, Medium-, and High-Tech Industries on Venture Performance and Survival," in *IEEE Transactions on Engineering Management*, vol. 68, no. 6, pp. 1907-1918, Dec. 2021, doi: 10.1109/TEM.2019.2943703.
- [3] Z. Wang and Y. Fan, "Monitoring performance indicator related industrial process monitoring with a monitoring index identification model," *Control Engineering Practice*, vol. 139, p. 105660, 2023, doi: 10.1016/j.conengprac.2023.105660.
- [4] M. Asrol, S. Wahyudi, C. Harito, D. N. Utama, and M. Syafrudin, "Improving Supplier Evaluation Model using Ensemble Method-Machine Learning for Food Industry," *Procedia Computer Science*, vol. 227, pp. 307-315, 2023, doi: 10.1016/j.procs.2023.10.529.
- [5] F. Yin, Y. Guo, Z. Qiu, H. Niu, W. Wang, Y. Li, and N. Y. Kim, "Hybrid electronic skin combining triboelectric nanogenerator and humidity sensor for contact and non-contact sensing," *Nano Energy*, vol. 101, p. 107541, 2022, doi: 10.1016/j.nanoen.2022.107541.
- [6] H. Xiao, D. McDonald, Y. Fan, P. B. Umbanhowar, J. M. Ottino, and R. M. Lueptow, "Controlling granular segregation using modulated flow," *Powder Technology*, vol. 312, pp. 360-368, 2017, doi: 10.1016/j.powtec.2017.02.050.
- [7] M. Nawaz, A. S. Maulud, H. Zabiri, and H. Suleman, "Review of Multiscale Methods for Process Monitoring, With an Emphasis on Applications in Chemical Process Systems," in *IEEE Access*, vol. 10, pp. 49708-49724, 2022, doi: 10.1109/ACCESS.2022.3171907.
- [8] P. M. B. Bugallo, A. Stupak, L. C. Andrade, and R. T. López, "Material Flow Analysis in a cooked mussel processing industry," *Journal of food engineering*, vol. 113, No. 1, pp. 100-117, 2012, doi: 10.1016/j.jfoodeng.2012.05.014.
- [9] N. N. Alves, G. B. Messaoud, S. Desobry, J. M. C. Costa, and S. Rodrigues, "Effect of drying technique and feed flow rate on bacterial survival and physicochemical properties of a non-dairy fermented probiotic juice powder," *Journal of Food Engineering*, vol. 189, pp. 45-54, 2016, doi: 10.1016/j.jfoodeng.2016.05.023.
- [10] D. Hawashin, K. Salah, R. Jayaraman, and A. Musamih, "Using Composable NFTs for Trading and Managing Expensive Packaged Products in the Food Industry," in *IEEE Access*, vol. 11, pp. 10587-10603, 2023, doi: 10.1109/ACCESS.2023.3241226.
- [11] J. Liu, R. An, R. Xiao, Y. Yang, G. Wang, and Q. Wang, "Implications from substance flow analysis, supply chain and supplier risk evaluation in iron and steel industry in Mainland China," *Resources Policy*, vol. 51, pp. 272-282, 2017, doi: 10.1016/j.resourpol.2017.01.002.
- [12] Y. Jia, Z. G. Zhang, and T. Xu, "Improving the Performance of MMPP/M/C Queue by Convex Optimization—A Real-World Application in Iron and Steel Industry," in *IEEE Access*, vol. 8, pp. 185909-185918, 2020, doi: 10.1109/ACCESS.2020.3030325.
- [13] R. B. Shah, M. A. Tawakkul, and M.A. Khan, "Comparative Evaluation of Flow for Pharmaceutical Powders and Granules," *AAPS PharmSciTech*, vol. 9, pp. 250-258, 2008, doi: 10.1208/s12249-008-9046-8.
- [14] Z. Wang *et al.*, "Adaptive Quality Control With Uncertainty for a Pharmaceutical Cyber-Physical System Based on Data and Knowledge

- Integration," in *IEEE Transactions on Industrial Informatics*, vol. 20, no. 3, pp. 3339-3350, March 2024, doi: 10.1109/TII.2023.3306355.
- [15] O. A. Odunlami, T. E. Amoo, H. A. Adisa, F. B. Elehinfafe, and T. E. Oladimeji, "Application of mass transfer in the pulp and paper Industry— overview, processing, challenges, and prospects," *Results in Engineering*, p. 101498, 2023, doi: 10.1016/j.rineng.2023.101498.
- [16] Z. Liu, L. Zhao, S. Lu, X. Hou, D. Hou, and J. Ma, "Porous ceramsite catalytic ozonation for the treatment of pulp and paper mill wastewater in a continuous-flow reactor," *Chemical Engineering Science*, p. 119855, 2024, doi: 10.1016/j.ces.2024.119855.
- [17] P. J. LaNasa and E. L. Upp. *Fluid Flow Measurement: A Practical Guide to Accurate Flow Measurement*. Butterworth-Heinemann, pp. 35-47, 2014.
- [18] O. Elijah *et al.*, "A Survey on Industry 4.0 for the Oil and Gas Industry: Upstream Sector," in *IEEE Access*, vol. 9, pp. 144438-144468, 2021, doi: 10.1109/ACCESS.2021.3121302.
- [19] W. Liu, J. Hu, X. Zhao, H. Pan, I. A. Lakhari, and W. Wang, "Development and experimental analysis of an intelligent sensor for monitoring seed flow rate based on a seed flow reconstruction technique," *Computers and Electronics in Agriculture*, vol. 164, p. 104899, 2019, doi: 10.1016/j.compag.2019.104899.
- [20] F. He, X. Ma, K. Shen, and C. Wang, "Study on Material and Energy Flow in Steel Forging Production Process," in *IEEE Access*, vol. 8, pp. 12921-12932, 2020, doi: 10.1109/ACCESS.2019.2958630.
- [21] S. Melzer, P. Munsch, J. Förster, J. Friderich, and R. Skoda, "A system for time-fluctuating flow rate measurements in a single-blade pump circuit," *Flow Measurement and Instrumentation*, vol. 71, p. 101675, 2020, doi: 10.1016/j.flowmeasinst.2019.101675.
- [22] J. Massaad *et al.*, "Measurement of Pipe and Fluid Properties With a Matrix Array-Based Ultrasonic Clamp-On Flow Meter," in *IEEE Transactions on Ultrasonics, Ferroelectrics, and Frequency Control*, vol. 69, no. 1, pp. 309-322, Jan. 2022, doi: 10.1109/TUFFC.2021.3111710.
- [23] S. S. Nair, V. Vinodkumar, V. Sreedevi, and D. S. Nagesh, "Design of electromagnetic probe having reduced base line drift for blood flow measurement," *IETE Journal of Research*, vol. 61, pp. 329-340, doi: 10.1080/03772063.2015.1018347.
- [24] J. P. Bentley. *Principles of Measurement Systems*. Pearson education, pp. 275-303, 2005.
- [25] J. Liu, H. Qi, Y. Song, S. Chen, and D. Wu, "Dynamics of bubbles detached from non-circular orifices: Confinement effect of orifice boundary," *Chemical Engineering Journal*, vol. 471, p. 144777, 2023, doi: 10.1016/j.cej.2023.144777.
- [26] S. K. Venkata and B. K. Roy, "A practically validated intelligent calibration circuit using optimized ANN for flow measurement by venturi," *Journal of The Institution of Engineers (India): Series B*, vol. 97, pp.31-39, 2016.
- [27] W. Chen, J. Li, Y. Li, M. Zhang, and L. Peng, "Flowrate Estimation of Horizontal Gas-Water Slug Flow Based on Venturi Tube and Conductance Sensor," in *IEEE Transactions on Instrumentation and Measurement*, vol. 70, pp. 1-10, 2021, doi: 10.1109/TIM.2021.3097398.
- [28] C. H. Lee, H. K. Jeon, and Y. S. Hong, "An implementation of ultrasonic water meter using dToF measurement," *Cogent Engineering*, vol. 4, p. 1371577, 2017, doi: 10.1080/23311916.2017.1371577.
- [29] Y. Zhao, Y. F. Gu, R. Q. Lv, and Y. Yang, "A small probe-type flowmeter based on the differential fiber Bragg grating measurement method," *IEEE Transactions on Instrumentation and Measurement*, vol. 66, pp. 502-507, 2017, doi: 10.1109/TIM.2016.2631779.
- [30] Z. Liu and W. Wang, "Flow measurement method based on a fringing field capacitor structure," *Electronics Letters*, vol. 52, pp. 1771-1772, 2016.
- [31] S. Sinha, D. Banerjee, N. Mandal, R. Sarkar, and S. C. Bera, "Design and implementation of real-time flow measurement system using Hall probe sensor and PC-based SCADA," *IEEE Sensors Journal*, vol. 15, no. 10, pp. 5592-5600, 2015, doi: 10.1109/JSEN.2015.2442651.
- [32] D. P. Lannes, A. L. Gama, and T. F. B. Bento, "Measurement of flow rate using straight pipes and pipe bends with integrated piezoelectric sensors," *Flow Measurement and Instrumentation*, vol. 60, pp. 208-216, 2018, doi: 10.1016/j.flowmeasinst.2018.03.001.
- [33] K. A. R. Medeiros, F. L. A. de Oliveira, C. R. H. Barbosa, and E. C. de Oliveira, "Optimization of flow rate measurement using piezoelectric accelerometers: Application in water industry," *Measurement*, vol. 91, pp. 576-581, 2016, doi: 10.1016/j.measurement.2016.05.101.
- [34] Q. Li, J. Xing, D. Shang, and Y. Wang, "A flow velocity measurement method based on a PVDF piezoelectric sensor," *Sensors*, vol. 19, p. 1657, 2019.
- [35] J. Krejčí, L. Ježová, R. Kučerová, R. Plička, Š. Broža, D. Krejčí, and I. Ventrubová, "The measurement of small flow, *Sensors and Actuators A: Physical*," vol. 266, pp. 308-313, 2017, doi: 10.1016/j.sna.2017.08.050.
- [36] J. Biswal, H. J. Pant, S. Goswami, J. S. Samantray, V. K. Sharma, and K. S. S. Sarma, "Measurement of flow rates of water in large diameter pipelines using radiotracer dilution method," *Flow Measurement and Instrumentation*, vol. 59, pp. 194-200, 2018, doi: 10.1016/j.flowmeasinst.2017.12.014.
- [37] M. Norgia, A. Pesatori, and S. Donati, "Compact laser-diode instrument for flow measurement," *IEEE Transactions on Instrumentation and Measurement*, vol. 65, pp. 1478-1483, 2016, doi: 10.1109/TIM.2016.2526759.
- [38] M. Arlit, C. Schroth, E. Schleicher, and U. Hampel, "Flow rate measurement in flows with asymmetric velocity profiles by means of distributed thermal anemometry," *Flow Measurement and Instrumentation*, vol. 68, p. 101570, 2019, doi: 10.1016/j.flowmeasinst.2019.05.004.
- [39] R. Cernat, A. Bradu, R. Rajendram, and A. G. Podoleanu, "Simultaneous measurement of flow at several depths using multiple active paths in a low-coherence interferometer," *IEEE Photonics Journal*, vol. 7, pp. 1-12, 2015.
- [40] A. Lay-Ekuakille, P. Vergallo, G. Griffio, and R. Morello, "Pipeline flow measurement using real-time imaging," *Measurement*, vol. 47, pp. 1008-1015, 2014, doi: 10.1016/j.measurement.2013.09.015.
- [41] L. Di Cecilia, S. Cattini, F. Giovanardi, and L. Rovati, "Single-arm self-mixing superluminescent diode interferometer for flow measurements," *Journal of Lightwave Technology*, vol. 35, pp. 3577-3583, 2016.
- [42] S. A. Mawjoud and I. Y. Dallal-Bashi, "Flow-Rate Measurements of Solid Particulates and Liquids Using Doppler Effect," *IETE Journal of Research*, vol. 28, pp. 597-601, 1982, doi: 10.1080/03772063.1982.11452846.
- [43] K. A. Atek, S. A. Mawjoud, and A. S. Jabber, "The Effect of Humidity and Bulk Density on Flow Rate Measurements of Rice, Salt and Sugar," *IETE Journal of Research*, vol. 30, pp. 124-128, 1984, doi: 10.1080/03772063.1984.11453254.
- [44] M. Javaid, A. Haleem, R. P. Singh, S. Rab, and R. Suman, "Significance of sensors for industry 4.0: Roles, capabilities, and applications," *Sensors International*, vol. 2, pp. 100110, 2021, doi: 10.1016/j.sintl.2021.100110.
- [45] L. Yao and Z. Ge, "Industrial Big Data Modeling and Monitoring Framework for Plant-Wide Processes," in *IEEE Transactions on Industrial Informatics*, vol. 17, no. 9, pp. 6399-6408, Sept. 2021, doi: 10.1109/TII.2020.3010562.
- [46] D. Mishra, R. B. Roy, S. Dutta, S. K. Pal, and D. Chakravarty, "A review on sensor based monitoring and control of friction stir welding process and a roadmap to Industry 4.0," *Journal of Manufacturing Processes*, vol. 36, pp. 373-397, 2018, doi: 10.1016/j.jmappro.2018.10.016.
- [47] F. Curreri, G. Fiumara, and M. G. Xibilia, "Input selection methods for soft sensor design: A survey," *Future Internet*, vol. 12, No. 6, p. 97, 2020, doi: 10.3390/fi12060097.
- [48] L. Fortuna, S. Graziani, A. Rizzo, and M. G. Xibilia, "Soft Sensors for Monitoring and Control of Industrial Processes," *UK: Springer*, vol. 22, 2007.
- [49] A. Q. Al Saedi and C. S. Kabir, "Estimation of heat-flow rate from fluid-flow rate," *Journal of Petroleum Science and Engineering*, vol. 191, p. 107203, 2020, doi: 10.1016/j.petrol.2020.107203.
- [50] X. Han, J. Jiang, A. Xu, X. Huang, C. Pei, and Y. Sun, "Fault Detection of Pneumatic Control Valves Based on Canonical Variate Analysis," in *IEEE Sensors Journal*, vol. 21, no. 12, pp. 13603-13615, 2021, doi: 10.1109/JSEN.2021.3070035.
- [51] S. Haddad, M. Benganem, A. Mellit, and K. O. Daffallah, "ANNs-based modeling and prediction of hourly flow rate of a photovoltaic

- water pumping system: Experimental validation,” *Renewable and Sustainable Energy Reviews*, vol. 43, pp. 635-643, 2015, doi: 10.1016/j.rser.2014.11.083.
- [52] J. Tomperi, P. M. Rossi, and M. Ruusunen, “Estimation of wastewater flowrate in a gravitational sewer line based on a low-cost distance sensor,” *Water Practice & Technology*, vol. 18, no. 1, pp. 40-52, 2023, doi: 10.2166/wpt.2022.171.
- [53] S. K. Venkata and B. R. Navada, “Estimation of flow rate through analysis of pipe vibration,” *acta mechanica et automatica*, vol. 12, pp. 294-300, 2018, doi: 10.2478/ama-2018-0045.
- [54] S. Hucko, H. Krampe, and K. Schmitz, “Evaluation of a Soft Sensor Concept for Indirect Flow Rate Estimation in Solenoid-Operated Spool Valves,” in *Actuators*, vol. 12, no. 4, p. 148, March 2023, doi: 10.3390/act12040148.
- [55] B. R. Navada, S. K. Venkata, and S. Rao, “A Soft Sensor for Estimation of In-Flow Rate in a Flow Process Using Pole Placement and Kalman Filter Methods,” *Machines*, vol. 7, p. 63, 2019, doi: 10.3390/machines7040063.
- [56] M. Khalid, L. Pénard, and E. Mémin, “Optical flow for image-based river velocity estimation,” *Flow Measurement and Instrumentation*, vol. 65, pp. 110-121, 2019, doi: 10.1016/j.flowmeasinst.2018.11.009.
- [57] M. T. Islam and R. Righetti, “A novel filter for accurate estimation of fluid pressure and fluid velocity using poroelastography,” *Computers in biology and medicine*, vol. 101, pp. 90-99, 2018, doi: 10.1016/j.compbiomed.2018.08.007.
- [58] F. Ejeian, S. Azadi, A. Razmjou, Y. Orooji, A. Kottapalli, M. E. Warkiani, and M. Asadnia, “Design and applications of MEMS flow sensors: A review,” *Sensors and Actuators A: Physical*, vol. 295, pp. 483-502, 2019, doi: 10.1016/j.sna.2019.06.020.
- [59] Y. K. Yaseen, A. H. Mhmood, M. R. Subhi, A. B. Rakan, and H. A. Mohammed, “Advanced Flowrate Control of Petroleum Products in Transportation: An Optimized Modified Model Reference PID Approach,” *Journal of Robotics and Control (JRC)*, vol. 4, no. 5, pp. 591-599, 2023.
- [60] B. R. Navada and S. Venkata, “Fusion-based online identification technique for pneumatic actuator faults,” *Engineered Science*, vol. 17, pp. 56-69, 2021.
- [61] J. Kodosky, “LabVIEW,” *Proceedings of the ACM on Programming Languages*, vol. 4, pp. 1-54, 2020.